Chemical Engineering Journal 431 (2022) 133475

Contents lists available at ScienceDirect

Chemical Engineering Journal

journal homepage: www.elsevier.com/locate/cej

Sustainable icephobicity on durable quasi-liquid surface

Jyotirmoy Sarma, Lei Zhang, Zongqi Guo, Xianming Dai *

Department of Mechanical Engineering, The University of Texas at Dallas, 800 W. Campbell Rd, Richardson, TX 75080, USA

ARTICLE INFO

Keywords:
Sustainable icephobicity
Ice adhesion
Quasi-liquid surface
Durability

ABSTRACT

Sustainable easy removal of accreted ice has been strongly desired worldwide. Passive anti-icing strategies relying on durable surface coatings are highly desired because of their simplicity and low cost compared to the energy-intensive active strategies. The current state-of-the-art anti-icing technologies, such as liquid-infused surfaces, are able to dramatically reduce ice adhesion strength. Nevertheless, severe durability challenges of lubricant depletion and coating damage during the ice removal process hinder their practical applications. Here, we report a quasi-liquid surface that can significantly reduce the ice adhesion strength by reducing the shear modulus of the coating. The quasi-liquid lubrication provided by the highly mobile chains of the flexible polymer changes the sticky ice/solid interface to a non-sticky ice/quasi-liquid interface. Moreover, each molecule chain is chemically bonded on the solid substrate so the entire surface can withstand abrasion in long-term de-icing conditions. The icephobicity on the quasi-liquid coating persists after chemical rinsing while the state-of-the-art liquid-infused surface fails due to lubricant depletion. In addition, we have demonstrated that controlling the shear modulus of an icephobic coating can achieve both small- and large-scale ice removal with the quasi-liquid approach. Such a durable quasi-liquid surface with sustainable ultralow shear strength shows a potential to reduce ice accretion on solar panels, power lines, and vehicles in ice prone regions.

1. Introduction

Ice accretion is one of the major challenges for power production and transportation in ice prone regions [1]. For example, the state of Texas in the United States came to a sudden standstill in February 2021 due to the unexpected snowstorm. Surface topography, surface chemistry and wetting behavior as well as ice characteristics have been reported to influence ice accretion and ice adhesion [2,3], indicating that studies on anti-icing are of utmost importance. Typically, active strategies (e.g., electrical heating elements, infrared hangars) and passive strategies (e.g., surface coatings) are used to tackle ice accretion. However, most of the active approaches are complex and costly. Hence, recent research has been focused on fundamental understanding of icing delay and ice removal on passive coatings. Delaying ice formation is a highly desired characteristic achieved through controlling ambient humidity and surface geometry [4,5], biphilic topography [6], solar thermal [7,8], incorporation of phase change materials [9], anti-freeze proteins [10] and nanomaterials [11]. The existence of bilayer ice on solid surfaces of different surface wettability governs the growth modes of ice crystals [12]. Icing can be delayed, but ice will eventually form on surfaces because of the ubiquitous dust and impurities in the environment which usually serve as undesired nucleation sites [11,13,14] and the existence of ice bridges [15]. Enabling easy ice removal after ice forms is another strategy to inhibit ice accretion. While the current state-of-the-art superhydrophobic surfaces [16–20], patterned surfaces [21,22], and liquid-infused surfaces [23,24] dramatically reduce ice adhesion strength, yet severe durability challenges of coating damage [25] and lubricant depletion [26] during ice removal hinder their practical applications. Therefore, developing sustainable icephobicity on a durable coating is highly desired.

The performance of an icephobic coating is typically evaluated by measuring the force, F, required to detach an ice block of a specified area, A, and is defined as ice adhesion strength [27], $\tau_{ice} = F/A$. A smaller ice adhesion strength indicates a better icephobicity. To achieve desired ultralow ice adhesion strength ($\tau_{ice} < 20$ kPa), ice must be removed from surfaces regardless of the size in long-term conditions. Large ice can be removed more easily than smaller one due to interfacial cracks. For instance, low interfacial toughness materials have recently been developed to remove meter-scale ice easily due to ice cracks at the interface [28]. This technique relies on a thin and high-modulus coating to yield low toughness. However, this technique is not effective for small ice removal. To induce interfacial cracks for small ice removal, an

* Corresponding author.
E-mail address: Dai@utdallas.edu (X. Dai).

https://doi.org/10.1016/j.cej.2021.133475
Received 14 August 2021; Received in revised form 31 October 2021; Accepted 2 November 2021
Available online 16 November 2021

elastomeric coating with internal airgaps is developed but it is not scalable [29].

An ideal icephobic coating must reduce ice adhesion strength for both large and small ice, as well as be durable and scalable. On icephobic coatings, ice adhesion strength depends on the work of adhesion between ice and the coating (W), shear modulus of the coating (μ) and the coating thickness (t). According to adhesion mechanics, the equation is shown below [30,31]

$$\tau_{ice} = \sqrt{\frac{\mu W}{t}} \quad (1)$$

The wettability of a surface can directly impact ice adhesion. Compared to a hydrophilic coating, a hydrophobic coating reduces the work of adhesion, W, and comparatively reduce τ_{ice} [1,27]. However, most of the rigid hydrophobic materials are known to exhibit a large ice adhesion strength ($\tau_{ice} > 100$ kPa) [27,32]. Soft hydrophobic materials can significantly reduce the ice adhesion strength but rely on thick coatings (i.e., large t), which are generally not scalable [33]. Reducing the interfacial shear modulus μ to nearly zero using liquid lubrication helps to achieve ultralow ice adhesion strength [24]. However, such liquid lubricated surfaces suffer from durability issues that result from lubricant depletion after several icing/de-icing cycles [26,34] or freezing of interfacial aqueous layer at low temperatures [35]. Organogels are able to maintain ultralow ice adhesion strength for a long duration due to lubricant infusion into their polymer networks which aids in interfacial slippage [33,36]. However, when cleaning or rinsing with chemicals is required (e.g., on airplane wings, solar panels, etc.), organogel coatings fail to maintain their icephobic property due to lubricant loss from the polymer networks. Hence, there has been a need for coatings with low shear modulus that can deliver ultralow ice adhesion strength as well as sustain such a low ice adhesion in various conditions. Quasi-liquid coating has shown liquid-like interface with ultrasmall shear modulus, so it can repel various chemicals with ultralow contact angle hysteresis (<1°) [37–39]. However, the durability of these quasi-liquid coatings under icing and deicing cycles are unexplored yet.

Sustainable ultralow ice adhesion on a durable quasi-liquid surface (QLS) along with scalable manufacture is strongly desired. In this work, we demonstrated sustainable icephobicity on QLS with ultralow ice adhesion strength. (1) A quasi-liquid surface can sustain its ultralow adhesion after harsh chemical rinsing. It remains effective for long term deicing after rigorous heat, water impingement and wiping tests. The thickness of the quasi-liquid coating is not a significant factor for achieving ice adhesion strength $\tau_{ice} < 20$ kPa, unlike those of soft coatings [33]. A thickness of approximately 4.5 nm quasi-liquid coating is enough to provide an ultralow shear modulus. (2) We also demonstrate that being a comparatively higher surface energy material, QLS yields a lower ice adhesion strength and a more durable icephobic performance than a perfluoroalkyl silane surface. (3) QLS can easily remove both small and large-scale ice, outperforming most icephobic surfaces. Along with anti-icing, sustainable energy harvesting in harsh conditions especially below sub-zero temperatures has always been a challenging problem [40,41]. We envision that the robust QLS with sustainable ultralow ice adhesion strength will provide design guidelines for sustainable anti-icing technologies in a harsh environment.

2. Experimental section

2.1. Materials

Silicone oil (i.e., trimethylsiloxy-terminated polydimethylsiloxane) with viscosities 20, 50, 100, 500, 1000, 5000, 30,000 and 100,000 cSt, and (tridecafluoro-1,1,2,2-tetrahydrooctyl)trichlorosilane (98%) were purchased from Gelest. Sylgard-184 silicone elastomer and heptane (99%) were purchased from Sigma-Aldrich and toluene (99.5%) from VWR. Plain glass slides 7.5 cm × 5.0 cm were purchased from Electron Microscopy Sciences, and large glass panes 15 cm × 10 cm from Amazon.com. Aluminum foils (thickness: 0.013 cm) were purchased from OnlineMetals.com, aluminum 6061 alloy sheets (thickness: 0.12 cm) from McMaster-Carr, and silicon wafers (diameter: 4 in.) from UniversityWafer. Polycarbonate tubes for fabricating cuvettes were purchased from McMaster-Carr. Windshield wiper blades (TRICO ExactFit, 12 in.) were purchased from Grainger. Deionized (DI) water, prepared by using a Milli-Q water purification system (Millipore), was used to form ice.

2.2. Fabrication of Quasi-liquid coating on various substrates

The quasi-liquid surface was made by tethering the flexible polymer of silicone oil (viscosity: 500 cSt) on a solid substrate with a one-step self-catalyzed grafting method through immersion in the solvent mixture of silicone oil and n-heptane in the ratio of 1:10 (Fig. S1) [42]. The substrates were immersed in the solution mixture for 48 h before rinsing with toluene to remove the lubricant layer from the surface. Specifically, the siloxane grafted substrates with excess silicone oil lubricant on the surface were immersed in a toluene bath and placed inside a shaker (100 rpm) for 2 min to ensure uniform rinsing. For the initial parametric studies for optimization of the viscosity of silicone oil for fabrication of QLS, the substrates were immersed only in pure silicone oil instead of the silicone oil-heptane mixture and the grafting time was 12 h. All the substrates in this study were washed with acetone and oxygen plasma treated (PX-250, March Asher) for 10 min at 200 W with 200 mTorr O_2 gas prior to immersion in the QLS solvent mixtures. However, it was also shown that pre-treatment with oxygen plasma is not necessary for fabricating a QLS on surfaces with inherent –OH groups (Fig. S2).

2.3. Fabrication of Lubricant-infused PDMS (Organogel)

The cross-linked PDMS substrate was fabricated on glass substrate using a mixture ratio of 10:1 for PDMS pre-polymer and cross-linking agent (Sylgard-184 silicone elastomer). The mixture was stirred by a mechanical stirrer for 10 min and kept inside a vacuum desiccator to remove bubbles. Then the mixture was spin-coated (2000 rpm, 30 s) onto a glass slide, followed by curing in a vacuum oven at 60 °C for 12 h. The cross-linked PDMS surface was then immersed in silicone oil (500 cSt) for 12 h to completely expand the PDMS network for lubricant infusion. This was followed by removal of the excess silicone oil from the surface using the spin-coater (2000 rpm, 30 s) to form the organogel surface.

2.4. Contact angle measurements

The contact angle measurements were carried out using a standard goniometer (Model 290, Rame-hart) at room temperature under ambient conditions (20–22 °C, ~40% relative humidity). All the contact angle values were averaged from at least 5 independent measurements by applying ~5 μL droplets on the test platform. For the measurement of contact angle hysteresis, the surface was tilted with respect to the horizontal plane until the liquid droplet started to slide along the surface. Then, advancing, receding, and sliding angles of the droplet were calculated by a computer program (Rame-hart DROPimage Advanced) in which the drops were fitted into a spherical cap.

2.5. Characterization

The thickness of the thin film of quasi-liquid surface was characterized using the Woollam M2000D Ellipsometer (WVASE32). An average of 3 measurements on each QLS sample grafted on silicon wafers were used to calculate the film thickness.

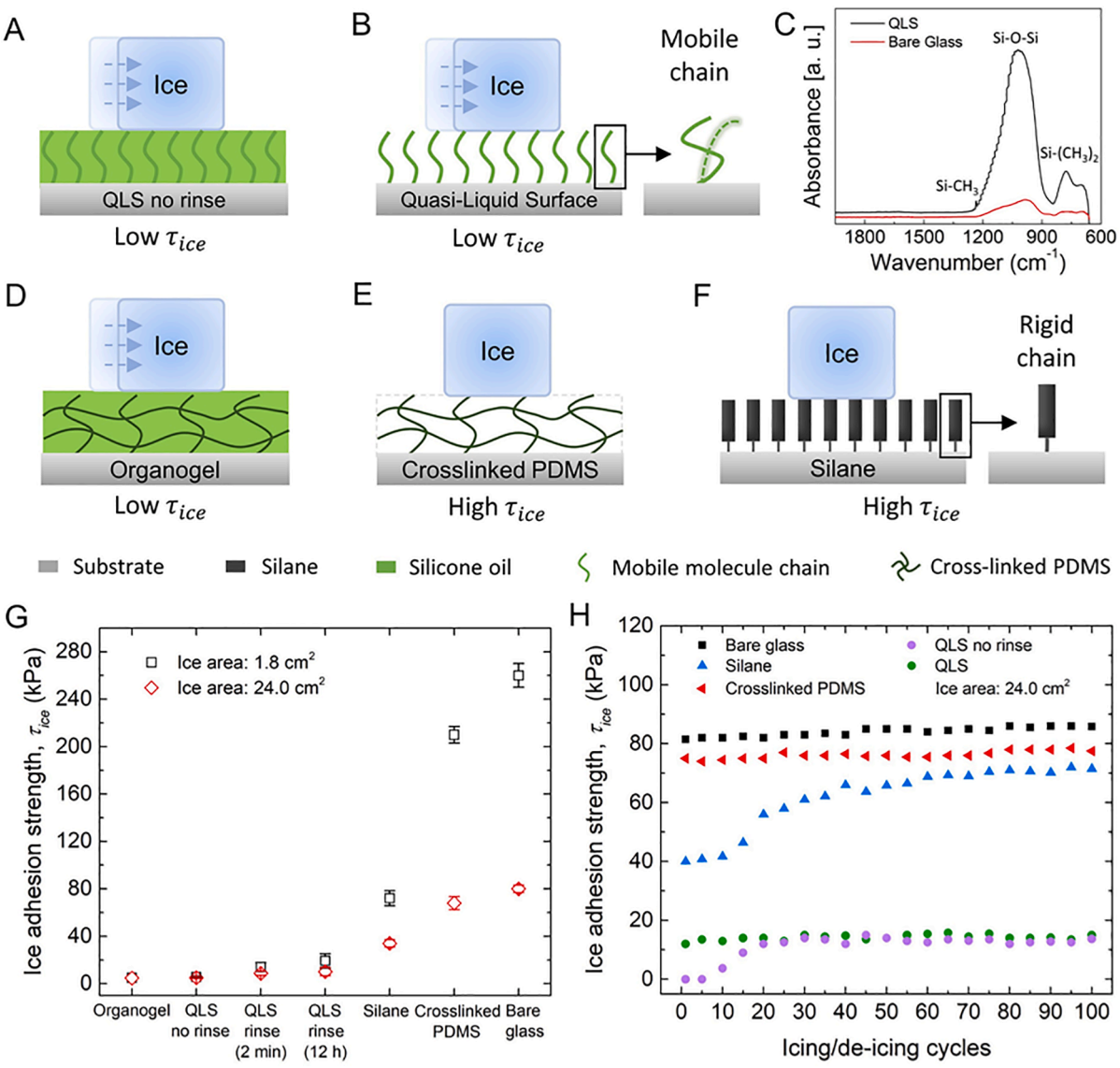

Fig. 1. Durable de-icing on quasi-liquid surface. Schematic showing low ice adhesion on (A) quasi-liquid surface without rinse, (B) quasi-liquid surface after rinsing with toluene showing mobile grafted chains of siloxane through (C) ATR-FTIR data and (D) organogel. Schematics showing (E) crosslinked PDMS with high ice adhesion due to crosslinked network, and (F) high adhesion and no durability on perfluoroalkyl silane, (G) comparison of ice adhesion strength of different surfaces with change in ice area and (H) de-icing performances of different surfaces over 100 icing/de-icing cycles.

2.6. De-icing test

The tests for ice removal were performed using a custom-built setup (Fig. S3-S4) described previously [37]. A force gauge (Nextech DFS500) with a resolution of 0.1 N was integrated on a syringe pump (PHD 2000, Harvard Apparatus), which provided precise movement for the force gauge maintaining the probe speed at 0.5 mm/s. The gauge probe pushes the ice adhered to the substrate placed on a Peltier plate (CP-200HT-TT, TE Technology, Inc.) maintained at a temperature of −10 °C. The thickness of ice in the cuvettes is ~1 to 1.3 cm. Deionized water was used for forming ice, and sufficient time was allowed for ice to freeze on the substrate before testing. Ice adhesion measurements were performed for 3 times successively on three different samples. Thus, the reported ice adhesion strength values are averaged over a total of 9 measurements.

2.7. Durability tests

The ice adhesion measurements for durability tests are the average of 3 successive measurements on three different samples. For the first experiment, the QLS and QLS no rinse samples on glass substrates were studied for durability by performing standard icing/de-icing cycles and were compared with fluorosilanized glass and bare glass. The tests were performed for 100 cycles of icing and consecutive de-icing, and the ice coverage area used was 24.0 cm^2.

Heating test – The QLS and QLS no rinse samples were heated at 60 °C for 2 h on a hot plate. This was followed by durability study for 100 cycles of icing/de-icing.

Water impingement test – The QLS no rinse sample was held under a water faucet for 30 min at a volume flow rate of 0.2 L/s, when most of the visible lubricant on the surface was washed away leaving a thin layer of lubricant residue. The QLS sample was then followed suit for 30 min. After this water impingement step, both substrates were studied for 100 cycles of icing/de-icing.

Wiper test – For its ultralow ice removal characteristics and excellent liquid repellency, the QLS may be coated successfully on the windshields of automobile. The wiping frequency of a regular windshield wiper in a car lies between 20 and 45 cycles per minute. Therefore, to replicate the

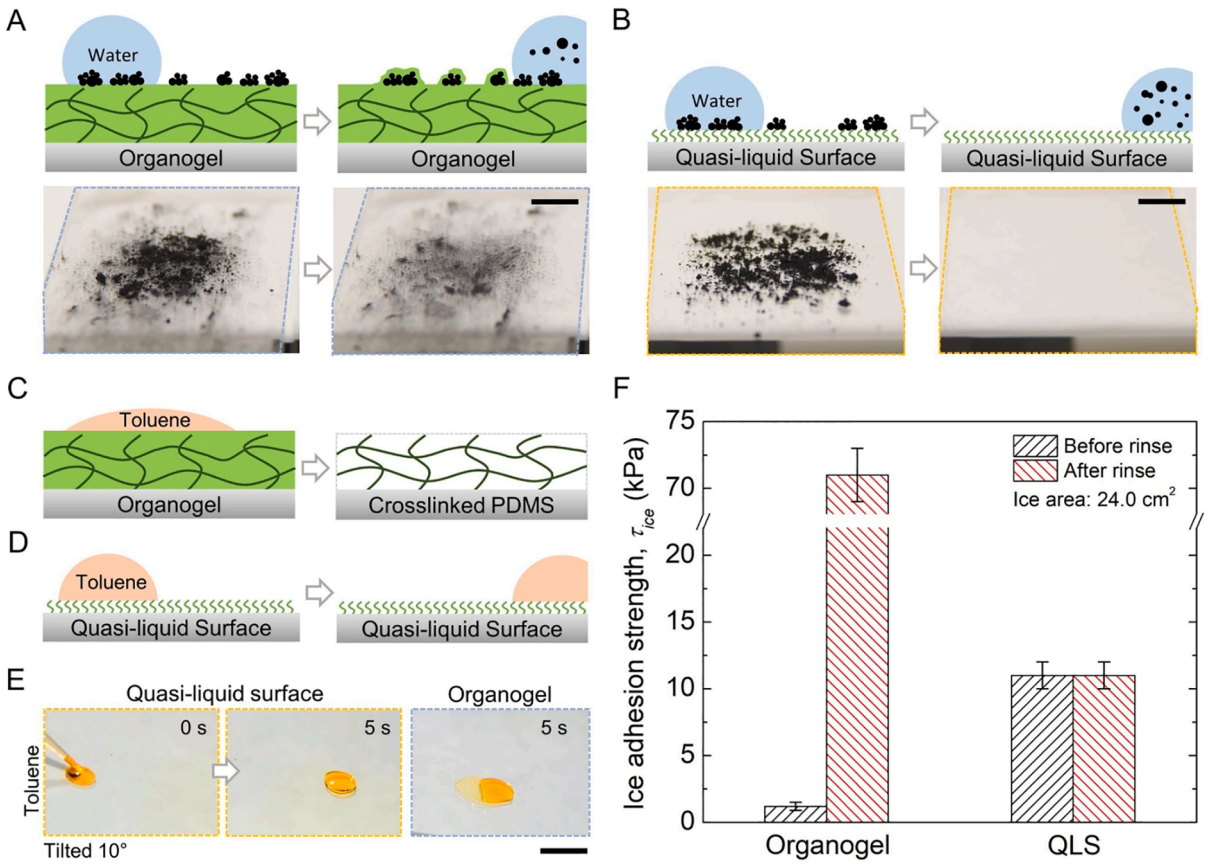

Fig. 2. Drawback of Organogel. Self-cleaning performance of (A) organogel compared to (B) QLS. Schematic showing (C) toluene wetting the organogel surface which readily gets converted to crosslinked PDMS after toluene rinse, and (D) toluene being repelled on the QLS. (E) Toluene repellency on QLS vs organogel. Toluene wets the organogel. (F) Ice adhesion strength performance of organogel and QLS before and after chemical rinse. Scale bars: (A), (B) and (E): 1 cm.

wiping on a car windshield, the QLS and QLS no rinse samples were wiped for 100 cycles at a frequency of 30 wiping cycles/min using a 12-inch windshield wiper (TRICO ExactFit). The samples were clamped on two sides during the process to keep them sturdy, and a pressure of 2.4 psi was applied to the windshield wiper. Then after the wiping for 100 cycles, it was followed by durability study for 100 cycles of icing/de-icing.

Chemical rinsing – The coated substrates were immersed in toluene, ethanol, and acetone subsequently for 2 min each in a shaker at 100 rpm, before being dried with compressed air.

3. Results and discussions

3.1. Quasi-liquid surface with de-icing durability

The quasi-liquid surface is fabricated by simply immersing a glass substrate with inherent hydroxyl groups into a solvent mixture of silicone oil and n-heptane in the ratio of 1:10. This resulted in a quasi-liquid surface infused with silicone oil (called as QLS no rinse) (Fig. 1A). When rinsing off the excess silicone oil with toluene, the flexible polymer brush is grafted on the solid substrate by tethering one end and keeping the other end mobile (Fig. 1B and 1C). Siloxane has been selected as the primary polymer chain due to its high thermal stability arising from the large bond energy (444 kJ mol^{-1}), as well as its inherent low surface energy from the hydrophobic methyl side groups, which also shields the inorganic Si-O backbone to lower intermolecular interactions within the molecule [42–44]. Hydrolysis of siloxane is followed by polycondensation with a surface silanol, specifically during hydrolysis the siloxane molecule undergoes scission by water molecules from the moisture. This is followed by grafting of the resulting compounds to the surface hydroxyl activated sites through polycondensation to form the quasi-liquid surface, and release of the water molecules back to the environment [42].

We made the state-of-the-art slippery liquid-infused porous surface (i.e., SLIPS) as a comparative study due to its low ice adhesion. Conventional SLIPS fail to sustain their ultralow ice adhesion strength due to depletion of the infused lubricant with each de-icing cycle [26]. Hence, organogel has served as a state-of-the-art SLIPS as it can maintain its ultralow ice adhesion strength. This is possible due to a low interfacial shear modulus which results from lubricant impregnation into the crosslinked networks of the polymer gel [33,36] (Fig. 1D). The free lubricant molecules provide interfacial slippage for ice removal [33]. However, they fail when the lubricant is displaced due to chemical rinsing with toluene. The infused liquid lubricant is dissolved and the organogel is readily converted to a crosslinked PDMS surface with restricted mobility (Fig. 1E). The extent of mobility of grafted polymer chains is significant for ice removal. This can be well understood from a silane surface's failure to yield low ice adhesion due to the rigid nature of its grafted molecular chains (Fig. 1F).

The quasi-liquid layer provides a good lubrication towards ice. QLS no rinse and QLS yield ice adhesion strength values of 0.5 kPa and 14 kPa respectively with sliding of ice on the surface effortlessly. We quantitively compared all the above-mentioned surfaces as shown in Fig. 1G. The forces required to remove a standard ice area (1.8 cm^2) from QLS 2 min rinse, QLS 12 h rinse, silane, crosslinked PDMS and bare glass are 25, 35, 130, 420 and 520 times higher than the QLS no rinse (0.5 kPa), respectively. Only organogel had a competitive performance due to its extrinsic liquid lubrication at the interface. When the ice coverage area was increased from 1.8 cm^2 to 24.0 cm^2, the ice adhesion strength was reduced due to internal ice cracks. However, for both small

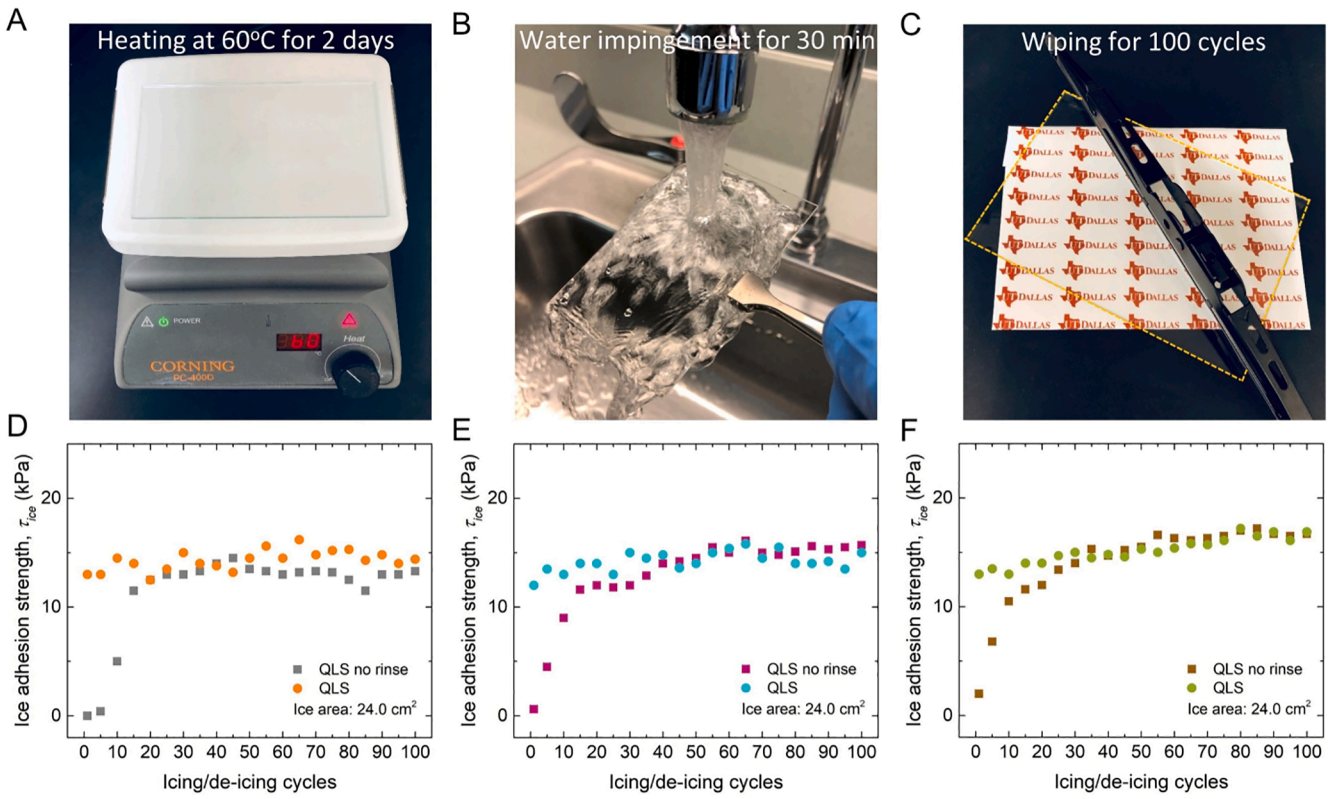

Fig. 3. Sustainable performance of quasi-liquid surface. (A) Heating of QLS on glass on a hot plate at 60 °C for 2 days, (B) water impingement on QLS on glass under a faucet for 30 min, (C) wiping of QLS on glass with a car windshield wiper for 100 consecutive cycles, (D) durable icephobic performance of QLS for 100 icing/de-icing cycles after heating test, (E) durable icephobic performance of QLS for 100 icing/de-icing cycles after water impingement test, and (F) durable icephobic performance of QLS for 100 icing/de-icing cycles after wiper test.

and large ice, organogel, QLS no rinse, and QLS show ultralow ice adhesion strength ($\tau_{ice} < 20$ kPa). As the ice adhesion strength for 2 min and 12 h rinse QLS samples show similar performances, we use the 2 min as rinsing time for all QLS samples.

Maintaining a long-term icephobic performance is a big challenge, although several icephobic coatings have been made to date. The failure mechanism includes: (i) the abrasion of the surface structures during de-icing, (ii) the depletion of liquid lubricant, or (iii) the rigidity of the grafted polymer films. Three coatings QLS, QLS no rinse and organogel showed promising results for long-term de-icing as they could maintain ultralow ice adhesion strength with τ_{ice} below 20 kPa after continuous icing/de-icing over 100 cycles (Fig. 1H). QLS no rinse showed 0.5 kPa ice adhesion strength during the initial icing/de-icing cycles, which gradually increased to 14 kPa until the visible lubricant film was completely depleted. QLS was exposed during continuous icing/de-icing. Therefore, the ultralow ice adhesion strength is sustained on QLS, unlike a conventional lubricant infused surface which loses its ultralow ice adhesion with the depletion of the lubricant overlayer [26,45]. Although organogel can retain liquid lubricant [33,46], it loses the slippery property, and hence icephobicity in harsh environments, which has been discussed extensively in the next section. As a control study for QLS, the silane coating showed a high ice adhesion strength (i.e., 40 kPa). Moreover, the silane surface gradually degraded and showed an increasing adhesion strength. This is attributed to the rigid molecular chain of the grafted silane. The quasi-liquid surface showed sustainable ultralow ice adhesion strength due to its exceptional durability.

3.2. Sustainability of quasi-liquid surface over organogel

The quasi-liquid surface offers sustainable icephobic performance over organogel in harsh environments. The organogel surface will fail when contaminated by dirt or in contact with organic solvents. From a practical standpoint, long-term usability of an icephobic organogel coating on a car windshield or solar panels does not seem feasible because organogel will eventually lose its liquid/ice repellency property due to contamination with dirt particles over time. Dirt particles get embedded into the top lubricant layer at the interface and a lubricant wrapping layer is formed, which makes it hard to self-clean the surface and results in increased surface roughness (Fig. 2A, Mov. S1). However, QLS coating is more favorable for a practical purpose as it can maintain its self-cleaning property throughout as shown in Fig. 2B. Dirt particles can easily be self-cleaned as there is no liquid layer on the surface.

Furthermore, the exposure to organic solvents like toluene, ethanol and acetone is detrimental to the slippery property of organogel. Toluene wets the organogel surface, dissolves all the lubricant in the networks and readily converts organogel to crosslinked PDMS (Fig. 2C). However, such a harsh chemical rinsing has no effect on QLS as it can repel these organic liquids (Fig. 2D). While a droplet of toluene spreads on an organogel surface, it can slide effortlessly on QLS (Fig. 2E). Loss of the liquid lubricant within organogel after harsh chemical rinsing has a significant impact on its icephobicity. The ice adhesion strength is increased by 140 times (Fig. 2F). On the other hand, there is no change in the ice adhesion strength on QLS as its quasi-liquid coating is unaffected by chemical rinsing.

Considering the practical applications of an icephobic coating, it will be exposed to sunlight, rain, and windshield wiper apart from chemicals. To further demonstrate the durability of QLS under such environments, we studied the sustainability of ultralow ice adhesion strength after (1) heating the substrate at 60 °C continuously for 2 days, (2) water impingement under a faucet for 30 min, and (3) 100 wiping cycles completed at a frequency of 30 wiping cycles per minute (Fig. 3A-C). This was followed by rigorous icing/de-icing up to 100 cycles for each of

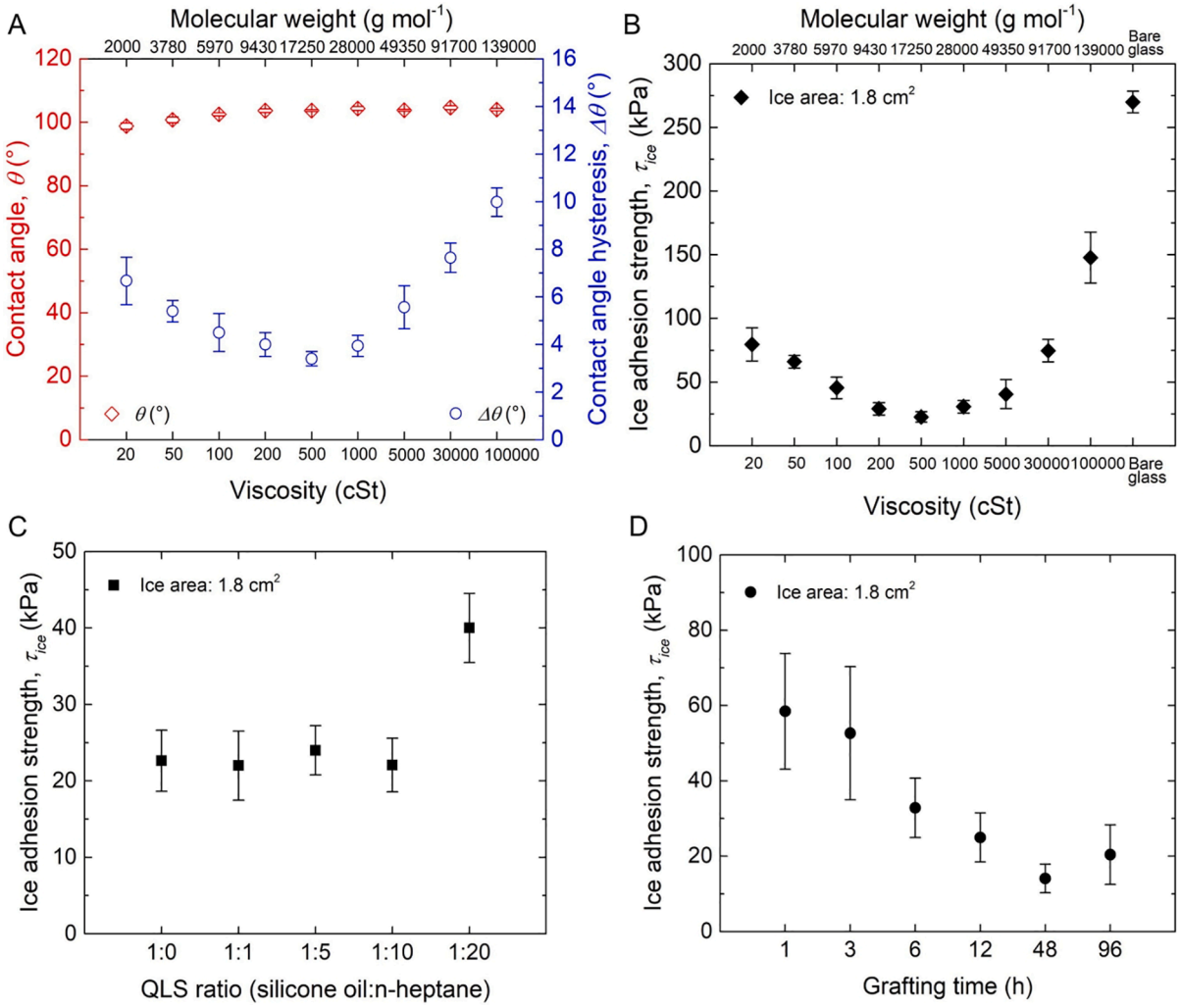

Fig. 4. Parametric optimization of quasi-liquid surface. (A) Wettability trend of QLS with different viscosities/molecular weights of silicone oil, (B) ice shearing trend of QLS with different viscosities/molecular weights of silicone oil, (C) comparison of ice adhesion strength for QLS (500 cSt) with different weight ratios of silicone oil to n-heptane, and (D) comparison of ice adhesion strength for different grafting time of QLS (500 cSt) with weight ratio 1:10.

the 3 test conditions. For all the three cases of heating, water impingement and wiper test, QLS maintained an ice adhesion strength of 14 ± 2 kPa after 100 icing/de-icing cycles (Fig. 3D-F). QLS no rinse showed an ultralow initial ice adhesion strength of 0.5 kPa due to the existence of lubricant overlayer. The ice adhesion strength increased gradually up to 12 kPa after 20 cycles of icing/de-icing, and then maintained at 14 ± 2 kPa after subsequent 100 cycles similar to the chemically rinsed QLS. The gradual increase in the ice adhesion strength up to 20 de-icing cycles can be attributed to the depletion of the lubricant overlayer with each cycle of deicing. However, after the depletion of the lubricant overlayer, QLS no rinse sample showed the same characteristics as the chemically rinsed QLS and sustained its ultralow ice adhesion strength. This also highlights that the quasi-liquid surface can address the durability challenges of liquid-infused surfaces and superhydrophobic surfaces in terms of long-term icephobicity. Furthermore, wettability test on the QLS for each of the heating, water impingement and wiper tests showed that there is no significant change in the water CA and CAH after 100 cycles of icing/de-icing (Fig. S5A-C). The water CA was maintained at 102° and CAH did not exceed 4°. The QLS is thermally stable at higher temperatures such as 250 °C (Fig. S7) due to the high bond dissociation energy (444 kJ/mol) of siloxane molecules covalently attached to the substrate [37].

QLS being a chemically grafted surface, a comparative study for 100 cycles of icing/deicing was done with a silane grafted control surface using ice area 1.8 cm^2. Silane coating was icephobic initially as it depicted an ice adhesion strength of around 65 kPa, however, the values kept on increasing with the subsequent deicing cycles and reached around 200 kPa after 100 cycles of icing/deicing (Fig. S8). The QLS still showed durable icephobicity with an ice adhesion strength maintained at 14 ± 2 kPa. The probable reason for such a trend is that the molecular chains of grafted silane are rigid in nature while that of QLS are very flexible due to the presence of Si-O-Si bonds which can maintain its elasticity throughout [47]. The rigid and flexible traits of silane and QLS respectively can be verified from the wettability plots in Fig. S9 which showed a clear drop in water CA by around 20° for the silane surface after 100 deicing cycles and a slight increase in the water CAH by around 3°.

3.3. Parametric optimization of the quasi-liquid surface

We used silicone oils with varying molecular weights to optimize the quasi-liquid surfaces. Silicone oils with molecular weights (MW) 2000, 3780, 5970, 9430, 17250, 28000, 49350, 91700, and 139000 g/mol i.e., corresponding viscosities 20, 50, 100, 200, 500, 1000, 5000, 30000, and 100,000 cSt, respectively, were used to make QLS with 12 h grafting time. Successful grafting of molecular chains with different molecular weights were verified as all of them could repel liquids like water, toluene, and acetone. The CA for water was maintained within 100-105°

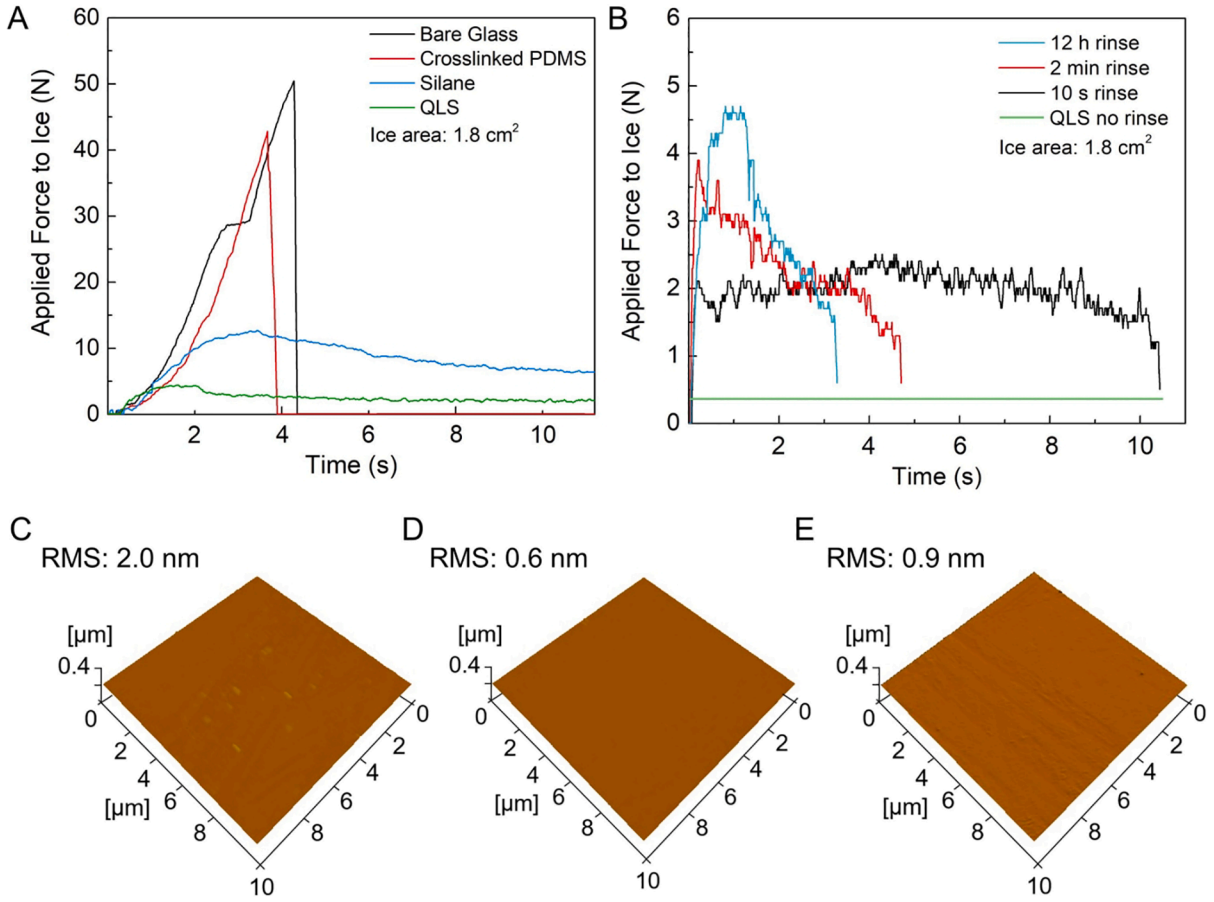

Fig. 5. Friction force on quasi-liquid surface. (A) Lateral force applied to ice on various surfaces reaches a critical value to overcome static friction and then either detaches or continues sliding with kinetic friction, and (B) fluctuations in the lateral force implies stick–slip behavior of the ice motion on QLS. 3D AFM images showing surface morphology of (C) bare glass, (D) QLS on glass, and (E) QLS after 100 cycles of de-icing.

across all the molecular weights, while CAH showed a decreasing trend from 2000 to 17250 g mol^{-1} and then increasing further (Fig. 4A). The lowest value for CAH was 3.5 ± 0.2° for molecular weight of silicone oil 17250 g mol^{-1} (viscosity: 500 cSt). The grafted surfaces of silicone oils with different molecular weights were then studied for de-icing. The shear strength for removal of ice was recorded lowest for molecular weight of silicone oil 17250 g mol^{-1} with a decreasing trend from 2000 to 17250 g mol^{-1} and then increasing further (Fig. 4B). When the molecular weight is low (i.e., <17250 g mol^{-1}), the substrate is not completely lubricated by the grafted polymer molecules. When the molecular weight is high (i.e., >17250 g mol^{-1}), the molecule chains are too long so they get entangled among themselves. With the increasing molecular weights, the complexity of the degree of molecular chain entanglement increases further. Hence, both CAH and ice adhesion strength follow the similar trend where the respective values decrease initially and then start increasing further. From this parametric optimization of the molecular weights, the silicone oil with molecular weight 17250 g mol^{-1} was fixed to be our optimized liquid for QLS fabrication.

To show the scalability and applicability of the QLS solvent on substrates of different shapes and sizes, silicone oil was mixed with n-heptane. The n-heptane mixes homogeneously with silicone oil by lowering its viscosity, which makes it suitable for use as a spray solvent, as well as an effortless rinsing with toluene. Solvent weight ratios for silicone oil to n-heptane were chosen as 1:0, 1:1, 1:5, 1:10 and 1:20 for an optimization study. There was no change in the ice adhesion strength (around 20 kPa) for all the weight ratios except for 1:20 (Fig. 4C). The strength value for 1:20 weight ratio was comparatively high (40 kPa). Also, there was a sharp decrease in the water CA value for weight ratio 1:20 followed by a comparatively large deviation in its CAH value (Fig. S10A). Therefore, the grafting of silicone oil molecular chains might not be uniform due to such a high weight ratio. The similar trend was observed for a volume ratio as well. Hence, considering the ease of applicability and limited usage of silicone oil to lower the cost, the weight ratio of 1:10 was chosen as the optimized solvent ratio for our QLS. Another important observation can be noted in terms of the grafting time. Ice adhesion strength kept on decreasing with the grafting time increased to 48 h (Fig. 4D). This is validated by the decreased CAH until 48 h of grafting time, after which the value of CAH increased (Fig. S10B). Such a change might possibly be due to increased grafting density of polymer chains, or increase in the molecular chain length with the grafting time until a certain chain length after which entanglement may occur. The complete removal of excess lubricant layer is achieved when the ice adhesion strength reaches a steady state with different rinsing time. With extensive rinsing time ranging from 2 min to 12 h, there was no significant deviation in the wettability and ice adhesion strength on the QLS (Fig. S11). Hence, 2 min rinse with toluene was used in this work if not specified. Therefore, considering all the parameters discussed above the optimized solvent and conditions for QLS fabrication were fixed as: molecular weight 17250 g mol^{-1}, silicone oil to n-heptane solvent weight ratio 1:10, grafting time 48 h and rinse time 2 min.

3.4. Mechanism of ultralow ice adhesion

The ultralow ice adhesion strength results from the small shear modulus of the quasi-liquid coating. The quasi-liquid surface with 4.5 ± 0.7 nm thickness is successful in robust long-term de-icing and maintains

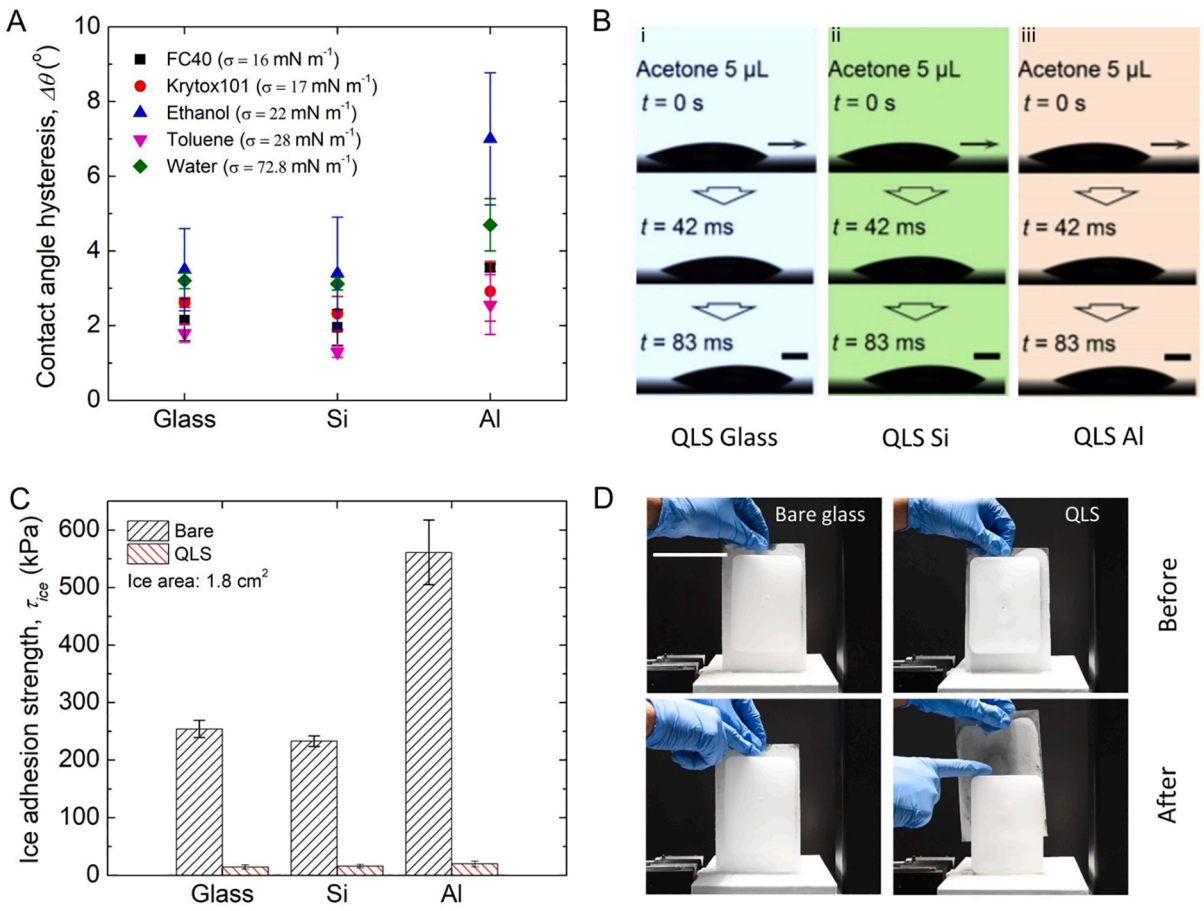

Fig. 6. Substrate independence of quasi-liquid surface and large ice removal. (A) Contact angle hysteresis data of liquids of various surface tension on QLS grafted on glass, silicon and aluminum, (B) repellency of acetone on QLS grafted on glass, silicon and aluminum, (C) comparison of ice adhesion strength on pristine bare substrates of glass, silicon and aluminum and their QLS grafted counterparts. (D) Demonstration of large-scale ice removal on bare glass and QLS coated glass. Ice area: 100.0 cm^2. Scale bars: (B) 1 mm, (D) 10 cm.

an ultralow ice adhesion strength below 20 kPa. Conventional technologies show that a thicker coating gives a better icephobic performance [33]. However, the thickness of the icephobic coating is not significant for achieving ultralow strength if the coating is in the liquid state. The grafted siloxane polymer brush has a low glass transition temperature (T_g = -125 °C) and low rotation barrier of Si-O-Si bond (bond angle = 143°) [37,42]. The siloxane is in the liquid state but each molecule is chemically bonded on the substrate, so it behaves as a quasi-liquid coating. On bare glass and crosslinked PDMS coating, ice detaches immediately from the surface as soon as the maximum force is applied. However, on the quasi-liquid surface, ice detaches after overcoming the maximum applied force and keeps sliding on the surface due to the kinetic friction (Fig. 5A). This is analogous to how a drop of liquid slides on a solid surface [48]. We found that the force required to overcome static friction followed by sliding due to kinetic friction in case of QLS is lower than that of silane. This can be attributed to the flexibility of the Si-O-Si backbone of QLS which is more mobile compared to the C–C–C backbone (bond angle = 109°) in that of silane [47,49]. Furthermore, the lateral friction force fluctuates in the kinetic regime until the ice is completely pushed off from QLS (Fig. 5B). This implies that there is a dynamic stick–slip motion of the ice on the QLS. It is usually observed when a rigid body is sliding on an elastic material with a low shear modulus [33,50,51]. Thus, the grafted mobile molecular chains of siloxane account for interfacial lubrication which is governed by an ultralow shear modulus of the quasi-liquid coating. The quasi-liquid surface is sustainable after hundreds of rigorous de-icing cycles due to the covalent bonding of the siloxane molecular chains to the substrate [37,42]. The QLS maintains its smooth surface morphology (Fig. 5C-E) because of the ultralow adhesion at the ice/quasi-liquid interface.

3.5. Substrate independence and large-scale ice removal

We have shown that a successful QLS fabrication can be achieved even without any prior surface activation (i.e., no plasma treatment). To demonstrate this, a pristine glass slide without prior plasma treatment was sprayed with the solvent mixture and let it stand for 48 h. Then, the excess lubricant on the surface was rinsed off with toluene for 2 min in a shaker. The surface made by the spray solvent showed water CA of 98.6 ± 2.1°, and CAH of 4.1 ± 0.4°. It could also repel perfluorinated liquids of ultralow surface tension like Krytox101 with a CAH of 3.0 ± 0.5° which demonstrated that QLS was fabricated successfully without prior surface activation. The ice adhesion strength on QLS fabricated without prior oxygen plasma treatment was around 2.5 times higher than that on a QLS pre-treated with oxygen plasma (Fig. S2), which is quite understandable because of limited activation sites on a substrate without plasma treatment. Nevertheless, the QLS fabricated without prior plasma treatment still yielded low ice adhesion (35 kPa). Apart from glass, the successful fabrication of QLS through liquid-phase method can be verified through facile repellency of various liquids with ultralow contact angle hysteresis. QLS fabricated on silicon and glass substrates show CAH as low as 2° for perfluorinated liquids like FC40 (γ = 16 mN m^{-1}) (Fig. 6A). The low surface tension liquid of acetone can also be repelled successfully on the QLS fabricated on glass, silicon and aluminum alike (Fig. 6B). However, the CAH could not be measured

successfully due to its high evaporation rate. The QLS fabricated through liquid-phase method yields an ultralow ice adhesion strength of 14 kPa regardless of the base substrate (Fig. 6C). Particularly, the ice adhesion strength was reduced by >90% on industrial aluminum materials. A coating that detaches readily from ice on a small surface does not necessarily mean that it can detach ice easily on a large surface [28]. Here we demonstrate that QLS not only is capable of removing small-sized ice, but also shows facile removal of large-scale iced areas up to 100 square centimeters (Fig. 6D, Mov. S2) which is usually hard to achieve with most icephobic coatings because the force required to remove ice from a surface usually scales up with the iced area.

4. Conclusions

We demonstrated that a quasi-liquid surface is the new state-of-the-art durable coating for sustainable and robust icephobicity under harsh conditions, such as heating, water impingement and wiping tests. It shows self-cleaning of dirt and repel chemicals, outperforming the organogel that fails in these conditions. Such an impressive icephobic performance of the quasi-liquid surface attributes to the ultrasoft interface with quasi-liquid lubrication provided by the mobile chains of the grafted flexible polymers. The liquid phase fabrication method is scalable and can be used for small- and large-scale ice removal alike. We found that a coating with nanometer thickness can yield ultralow ice adhesion strength by reducing the shear modulus of the interface. The ice adhesion strength on the quasi-liquid surface is much lower than that on a silane surface. More importantly, the durability and scalability of QLS addresses the major concern for most of the prior passive icephobic coatings when it comes to practical applications in daily life, such as solar panels, vehicle windshields, power lines, etc. The scalable applicability on industrial metals like aluminum will provide potential sustainable coatings for icephobicity.

Declaration of Competing Interest

The authors declare that they have no known competing financial interests or personal relationships that could have appeared to influence the work reported in this paper.

Acknowledgements

The authors gratefully acknowledge the startup funding support by the University of Texas at Dallas (UT Dallas), the Young Investigator Program at Army Research Office (Award No. W911NF1910416), and the National Science Foundation Faculty Early Career Development Program (Award No. 2044348) and Major Research Instrumentation Program (Award No. 2018188). This project was partially funded by the Office of Research at UT Dallas through the Core Facility Voucher Program. The authors would like to thank Dr. Li Shan, Fangying Chen and Deepak Monga for their help in characterizing the data.

Appendix A. Supplementary data

Supplementary data to this article can be found online at https://doi.org/10.1016/j.cej.2021.133475.

References

[1] L. Makkonen, Ice Adhesion —Theory, Measurements and Countermeasures, J. Adhes. Sci. Technol. 26 (4–5) (2012) 413–445, https://doi.org/10.1163/016942411X574583.
[2] S. Rønneberg, C. Laforte, C. Volat, J. He, Z. Zhang, The effect of ice type on ice adhesion, AIP Adv. 9 (5) (2019) 055304, https://doi.org/10.1063/1.5086242.
[3] S. Rønneberg, J. He, Z. Zhang, The need for standards in low ice adhesion surface research: a critical review, J. Adhes. Sci. Technol. 34 (3) (2020) 319–347, https://doi.org/10.1080/01694243.2019.1679523.
[4] Y. Yao, T.Y. Zhao, C. Machado, E. Feldman, N.A. Patankar, K.-C. Park, Frost-free zone on macrotextured surfaces, Proc. Natl. Acad. Sci. U.S.A. 117 (12) (2020) 6323–6329, https://doi.org/10.1073/pnas.1915959117.
[5] T.M. Schutzius, S. Jung, T. Maitra, P. Eberle, C. Antonini, C. Stamatopoulos, D. Poulikakos, Physics of icing and rational design of surfaces with extraordinary icephobicity, Langmuir 31 (17) (2015) 4807–4821, https://doi.org/10.1021/la502586a.
[6] Y. Hou, M. Yu, Y. Shang, P. Zhou, R. Song, X. Xu, X. Chen, Z. Wang, S. Yao, Suppressing ice nucleation of supercooled condensate with biphilic topography, Phys. Rev. Lett. 120 (7) (2018), 075902, https://doi.org/10.1103/PhysRevLett.120.075902.
[7] E. Mitridis, T.M. Schutzius, A. Sicher, C.U. Hail, H. Eghlidi, D. Poulikakos, Metasurfaces leveraging solar energy for icephobicity, ACS nano 12 (7) (2018) 7009–7017, https://doi.org/10.1021/acsnano.8b02719.
[8] W. Ma, Y. Li, C.Y.H. Chao, C.Y. Tso, B. Huang, W. Li, S. Yao, Solar-assisted icephobicity down to− 60° C with superhydrophobic selective surfaces, Cell Rep. Phys. Sci. 2 (3) (2021) 100384, https://doi.org/10.1016/j.xcrp.2021.100384.
[9] R. Chatterjee, D. Beysens, S. Anand, Delaying Ice and Frost Formation Using Phase-Switching Liquids, Adv. Mater. 31 (17) (2019) 1807812, https://doi.org/10.1002/adma.201807812.
[10] Z. He, K. Liu, J. Wang, Bioinspired Materials for Controlling Ice Nucleation, Growth, and Recrystallization, Acc. Chem. Res. 51 (5) (2018) 1082–1091, https://doi.org/10.1021/acs.accounts.7b00528.
[11] G. Bai, D. Gao, Z. Liu, X. Zhou, J. Wang, Probing the critical nucleus size for ice formation with graphene oxide nanosheets, Nature 576 (7787) (2019) 437–441, https://doi.org/10.1038/s41586-019-1827-6.
[12] J. Liu, C. Zhu, K. Liu, Y. Jiang, Y. Song, J.S. Francisco, X.C. Zeng, J. Wang, Distinct ice patterns on solid surfaces with various wettabilities, Proc. Natl. Acad. Sci. U.S.A. 114 (43) (2017) 11285–11290, https://doi.org/10.1073/pnas.1712829114.
[13] N.H. Fletcher, Size Effect in Heterogeneous Nucleation, J. Chem. Phys. 29 (3) (1958) 572–576, https://doi.org/10.1063/1.1744540.
[14] A. Welti, F. Lüönd, O. Stetzer, U. Lohmann, Influence of particle size on the ice nucleating ability of mineral dusts, Atmos. Chem. Phys. 9 (18) (2009) 6705–6715, https://doi.org/10.5194/acp-9-6705-2009.
[15] J.B. Boreyko, C.P. Collier, Delayed frost growth on jumping-drop superhydrophobic surfaces, ACS nano 7 (2) (2013) 1618–1627, https://doi.org/10.1021/nn3055048.
[16] L. Cao, A.K. Jones, V.K. Sikka, J. Wu, D. Gao, Anti-Icing Superhydrophobic Coatings, Langmuir 25 (21) (2009) 12444–12448, https://doi.org/10.1021/la902882b.
[17] J. Sarma, Z. Guo, X. Dai, Bioinspired photocatalytic hedgehog coating for super liquid repellency, Mater. Chem. Front. 5 (11) (2021) 4174–4181, https://doi.org/10.1039/D1QM00325A.
[18] S. Bengaluru Subramanyam, V. Kondrashov, J. Rühe, K.K. Varanasi, Low Ice Adhesion on Nano-Textured Superhydrophobic Surfaces under Supersaturated Conditions, ACS Appl. Mater. Interfaces 8 (20) (2016) 12583–12587, https://doi.org/10.1021/acsami.6b01133.
[19] S. Wu, Y. Du, Y. Alsaid, D. Wu, M. Hua, Y. Yan, B. Yao, Y. Ma, X. Zhu, X. He, Superhydrophobic photothermal icephobic surfaces based on candle soot, Proc. Natl. Acad. Sci. U.S.A. 117 (21) (2020) 11240–11246, https://doi.org/10.1073/pnas.2001972117.
[20] H. Zhang, G. Zhao, S. Wu, Y. Alsaid, W. Zhao, X. Yan, L. Liu, G. Zou, J. Lv, X. He, Solar anti-icing surface with enhanced condensate self-removing at extreme environmental conditions, Proc. Natl. Acad. Sci. U.S.A. 118(18) (2021). https://doi.org/10.1073/pnas.2100978118.
[21] S.F. Ahmadi, S. Nath, G.J. Iliff, B.R. Srijanto, C.P. Collier, P. Yue, J.B. Boreyko, Passive antifrosting surfaces using microscopic ice patterns, ACS Appl. Mater. Interfaces 10 (38) (2018) 32874–32884, https://doi.org/10.1021/acsami.8b11285.
[22] J.B. Boreyko, R.R. Hansen, K.R. Murphy, S. Nath, S.T. Retterer, C.P. Collier, Controlling condensation and frost growth with chemical micropatterns, Sci. Rep. 6 (1) (2016) 1–15, https://doi.org/10.1038/srep19131.
[23] T.-S. Wong, S.H. Kang, S.K.Y. Tang, E.J. Smythe, B.D. Hatton, A. Grinthal, J. Aizenberg, Bioinspired self-repairing slippery surfaces with pressure-stable omniphobicity, Nature 477 (7365) (2011) 443–447, https://doi.org/10.1038/nature10447.
[24] P. Kim, T.-S. Wong, J. Alvarenga, M.J. Kreder, W.E. Adorno-Martinez, J. Aizenberg, Liquid-Infused Nanostructured Surfaces with Extreme Anti-Ice and Anti-Frost Performance, ACS Nano 6 (8) (2012) 6569–6577, https://doi.org/10.1021/nn302310q.
[25] K.K. Varanasi, T. Deng, J.D. Smith, M. Hsu, N. Bhate, Frost formation and ice adhesion on superhydrophobic surfaces, Appl. Phys. Lett. 97 (23) (2010) 234102, https://doi.org/10.1063/1.3524513.
[26] K. Rykaczewski, S. Anand, S.B. Subramanyam, K.K. Varanasi, Mechanism of Frost Formation on Lubricant-Impregnated Surfaces, Langmuir 29 (17) (2013) 5230–5238, https://doi.org/10.1021/la400801s.
[27] A.J. Meuler, J.D. Smith, K.K. Varanasi, J.M. Mabry, G.H. McKinley, R.E. Cohen, Relationships between Water Wettability and Ice Adhesion, ACS Appl. Mater. Interfaces 2 (11) (2010) 3100–3110, https://doi.org/10.1021/am1006035.
[28] K. Golovin, A. Dhyani, M.D. Thouless, A. Tuteja, Low–interfacial toughness materials for effective large-scale deicing, Science 364 (6438) (2019) 371–375, https://doi.org/10.1126/science.aav1266.
[29] Z. He, S. Xiao, H. Gao, J. He, Z. Zhang, Multiscale crack initiator promoted super-low ice adhesion surfaces, Soft Matter 13 (37) (2017) 6562–6568, https://doi.org/10.1039/C7SM01511A.

[30] K. Kendall, The adhesion and surface energy of elastic solids, J. Phys. D Appl. Phys. 4 (8) (1971) 1186–1195, https://doi.org/10.1088/0022-3727/4/8/320.
[31] M.K. Chaudhury, K.H. Kim, Shear-induced adhesive failure of a rigid slabin contact with a thin confined film, Eur. Phys. J. E 23 (2) (2007) 175–183, https://doi.org/10.1140/epje/i2007-10171-x.
[32] W. Bascom, R. Cottington, C. Singleterry, Ice adhesion to hydrophilic and hydrophobic surfaces, J. Adhes. 1 (4) (1969) 246–263, https://doi.org/10.1080/00218466908072188.
[33] D.L. Beemer, W. Wang, A.K. Kota, Durable gels with ultra-low adhesion to ice, J. Mater. Chem. A 4 (47) (2016) 18253–18258, https://doi.org/10.1039/C6TA07262C.
[34] Q. Liu, Y. Yang, M. Huang, Y. Zhou, Y. Liu, X. Liang, Durability of a lubricant-infused electrospray silicon rubber surface as an anti-icing coating, Appl. Surf. Sci. 346 (2015) 68–76, https://doi.org/10.1016/j.apsusc.2015.02.051.
[35] Z. He, C. Wu, M. Hua, S. Wu, D. Wu, X. Zhu, J. Wang, X. He, Bioinspired Multifunctional Anti-icing Hydrogel, Matter 2 (3) (2020) 723–734, https://doi.org/10.1016/j.matt.2019.12.017.
[36] Y. Wang, X. Yao, J. Chen, Z. He, J. Liu, Q. Li, J. Wang, L. Jiang, Organogel as durable anti-icing coatings, Sci. China Mater. 58 (7) (2015) 559–565, https://doi.org/10.1007/s40843-015-0069-7.
[37] L. Zhang, Z. Guo, J. Sarma, X. Dai, Passive Removal of Highly Wetting Liquids and Ice on Quasi-Liquid Surfaces, ACS Appl. Mater. Interfaces 12 (17) (2020) 20084–20095, https://doi.org/10.1021/acsami.0c02014.
[38] L. Wang, T.J. McCarthy, Covalently Attached Liquids: Instant Omniphobic Surfaces with Unprecedented Repellency, Angew. Chem. Int. Edit. 55 (1) (2016) 244–248, https://doi.org/10.1002/anie.201509385.
[39] P. Liu, H. Zhang, W. He, H. Li, J. Jiang, M. Liu, H. Sun, M. He, J. Cui, L. Jiang, X. Yao, Development of "liquid-like" copolymer nanocoatings for reactive oil-repellent surface, ACS nano 11 (2) (2017) 2248–2256, https://doi.org/10.1021/acsnano.7b00046.
[40] Q. Zheng, Y. Jin, Z. Liu, H. Ouyang, H.u. Li, B. Shi, W. Jiang, H. Zhang, Z. Li, Z. L. Wang, Robust multilayered encapsulation for high-performance triboelectric nanogenerator in harsh environment, ACS Appl. Mater. Interfaces 8 (40) (2016) 26697–26703, https://doi.org/10.1021/acsami.6b06866.
[41] D. Bao, Z. Wen, J. Shi, L. Xie, H. Jiang, J. Jiang, Y. Yang, W. Liao, X. Sun, An anti-freezing hydrogel based stretchable triboelectric nanogenerator for biomechanical energy harvesting at sub-zero temperature, J. Mater. Chem. A 8 (27) (2020) 13787–13794, https://doi.org/10.1039/D0TA03215H.
[42] J.W. Krumpfer, T.J. McCarthy, Rediscovering Silicones: "Unreactive" Silicones React with Inorganic Surfaces, Langmuir 27 (18) (2011) 11514–11519, https://doi.org/10.1021/la202583w.
[43] H. Teisala, P. Baumli, S.A.L. Weber, D. Vollmer, H.-J. Butt, Grafting Silicone at Room Temperature—a Transparent, Scratch-resistant Nonstick Molecular Coating, Langmuir 36 (16) (2020) 4416–4431, https://doi.org/10.1021/acs.langmuir.9b03223.
[44] Y. Zhuo, S. Xiao, A. Amirfazli, J. He, Z. Zhang, Polysiloxane as icephobic materials – The past, present and the future, Chem. Eng. J. 405 (2021) 127088, https://doi.org/10.1016/j.cej.2020.127088.
[45] K. Golovin, S.P.R. Kobaku, D.H. Lee, E.T. DiLoreto, J.M. Mabry, A. Tuteja, Designing durable icephobic surfaces, Sci. Adv. 2 (3) (2016), e1501496, https://doi.org/10.1126/sciadv.1501496.
[46] J. Cui, D. Daniel, A. Grinthal, K. Lin, J. Aizenberg, Dynamic polymer systems with self-regulated secretion for the control of surface properties and material healing, Nat. Mater. 14 (8) (2015) 790–795, https://doi.org/10.1038/nmat4325.
[47] L. Zhang, Z. Guo, J. Sarma, W. Zhao, X. Dai, Gradient Quasi-Liquid Surface Enabled Self-Propulsion of Highly Wetting Liquids, Adv. Funct. Mater. 31 (13) (2021) 2008614, https://doi.org/10.1002/adfm.202008614.
[48] N. Gao, F. Geyer, D.W. Pilat, S. Wooh, D. Vollmer, H.-J. Butt, R. Berger, How drops start sliding over solid surfaces, Nat. Phys. 14 (2) (2018) 191–196, https://doi.org/10.1038/nphys4305.
[49] S. Huang, J. Li, L. Liu, L. Zhou, X. Tian, Lossless Fast Drop Self-Transport on Anisotropic Omniphobic Surfaces: Origin and Elimination of Microscopic Liquid Residue, Adv. Mater. 31 (27) (2019) 1901417, https://doi.org/10.1002/adma.201901417.
[50] H. Yoshizawa, J. Israelachvili, Fundamental mechanisms of interfacial friction. 2. Stick-slip friction of spherical and chain molecules, J. Phys. Chem. 97 (43) (1993) 11300–11313, https://doi.org/10.1021/j100145a031.
[51] L. Xue, J.T. Pham, J. Iturri, A. del Campo, Stick–slip friction of PDMS surfaces for bioinspired adhesives, Langmuir 32 (10) (2016) 2428–2435, https://doi.org/10.1021/acs.langmuir.6b00513.